Inorg. Chem. **2003**, *42*, 2405–2409

Nanostructured Magnetic Cuprate Cluster: Synthesis, Structure, UV–Vis Spectroscopy, and Magnetic Properties of a New Copper(II) Arsenate $NaCuAsO_4$ Containing Discrete $[Cu_4O_{16}]^{24-}$ Clusters

Mutlu Ulutagay-Kartin,[†] Shiou-Jyh Hwu,*[,†] and Jeffrey A. Clayhold[‡]

Department of Chemistry, Clemson University, Clemson, South Carolina 29634-0973, and Department of Physics and Astronomy, Clemson University, Clemson, South Carolina 29634-1911

Received November 9, 2002

Crystals of copper(II) arsenate $NaCuAsO_4$ were grown by conventional high-temperature, solid-state methods in molten-salt media. The compounds were characterized by single crystal X-ray diffraction, UV–vis spectroscopy, and magnetic susceptibility measurements. $NaCuAsO_4$ crystallizes in a monoclinic lattice with $a = 6.002$ (1) Å, $b = 10.853$ (2) Å, $c = 10.373$ (2) Å, $\beta = 91.50$ (3)°, and $V = 675.4(2)$ Å^3; $P2_1/c$ (No. 14); $Z = 8$. The newly isolated sodium copper(II) arsenate reveals a pseudo-one-dimensional channel structure where the sodium cations reside. The extended framework contains nanostructured $[Cu_4O_{16}]^{24-}$ magnetic clusters that are interlinked by closed-shell, nonmagnetic AsO_4^{3-} oxy anions via sharing vertex oxygen atoms of the CuO_5 and AsO_4 polyhedral units. Each $[Cu_4O_{16}]^{24-}$ cluster consists of four CuO_5 square pyramidal units in a chair configuration centered by a center of inversion. The two crystallographically independent Cu^{2+} cations adopt the [4 + 1] CuO_5 Jahn–Teller distortion giving rise to an intense d–d transition in UV–vis absorption spectra. The magnetic susceptibility measurements reveal that the title compound is antiferromagnetic. At high temperatures, the data follows a pure Curie law, suggesting noninteracting spins, but with a rapid suppression of the effective spin below $T = 70$ K. At low temperature, the susceptibility collapses, indicating spin gap formation as the magnetic-cluster material settles into the lowest energy magnetic singlet state. The current work in the exploratory synthesis of oxy compounds containing nanostructured transition-metal-oxide magnetic clusters leads to new materials for experimental and theoretical developments of magnetic models.

Introduction

Transition metal (TM) oxy compounds are of great interest for their structural versatility. It is evident that structurally isolated TM-oxide clusters, chains, and layers incorporated in a three-dimensional lattice often mimic the unit structure of the bulk oxides of technological importance.[1] These solids are generally insulators, and due to the simplified (nanostructured) TM-oxide frameworks, their magnetic behavior can be interpreted more easily than that of bulk. Oxy compounds of this kind, therefore, could provide useful materials for experimental and theoretical developments of magnetic models.[2]

In general, oxy compounds of the first-row transition metals exhibit a wide range of interesting chemical and physical properties such as ion-exchange, ionic conductivity, catalysis, nonlinear optical properties, and magnetic ordering.[3] Since we are interested in systems that are of electronic and magnetic importance, we have paid special attention to the compound formation with middle (Mn) and late (Cu) transition metal cations that adopt multiple oxidation states. Thus far, the phosphates and arsenates discovered in our research laboratories are $Na_2MnP_2O_7$, $NaCsMnP_2O_7$, $NaCsMn_{0.35}Cu_{0.65}P_2O_7$,[4] $NaMnAsO_4$,[5] $AMn_4(AsO_4)_3$ (A = Na, K,[6]

* Corresponding author. E-mail: shwu@clemson.edu.
† Department of Chemistry.
‡ Department of Physics and Astronomy.

(1) (a) Hwu, S.-J. *Chem. Mater.* **1998**, *10*, 2846−2859. (b) Papaefthymiou G. C. *Phys. Rev. B* **1992**, *46* (16), 10366−10375.

(2) For example: (a) Snyder, J.; Slusky, J. S.; Cava, R. J.; Schiffer, P. *Nature* **2001**, *413*, 48−51. (b) Koo, H. J.; Whangbo, M. H. *Inorg. Chem.* **2000**, *39* (16), 3599−3604. (c) Goodenough, J. B. *Annu. Rev. Mater. Sci.* **1998**, *28*, 1−27. (d) Goodenough, J. B.; Zhou, J. S. *Chem. Mater* **1998**, *10* (10), 2980−2993. (e) Tressaud, A.; Dance, J.-M. *Struct. Bonding (Berlin)* **1982**, *52*, 87−146.

(3) (a) Aranda, M. A. G.; Attfield, J. P.; Bruque, S.; von Dreele, R. B. *J. Chem. Soc., Chem. Commun.* **1994**, 155−156. (b) Buckley, A. M.; Bramwell, S. T.; Visser, D.; Day, P. *J. Solid State Chem.* **1987**, *69*, 240−251. (c) Padhi, A. K.; Nanjundaswamy, K. S.; Goodenough, J. B. *J. Electrochem. Soc.* **1997**, *144* (4), 1188−1194. (d) Satyanarayan, M. N.; Deepthy, A.; Bhat, H. L. *Crit. Rev. Solid State Mater. Sci.* **1999**, *24* (2), 103−191.

10.1021/ic026169q CCC: $25.00
Published on Web 02/26/2003

Rb[7]), β-$NaCuPO_4$,[5] $Na_2CuP_2O_7$,[8] $LiCu_2PO_5$,[9] $Ba_2Cu(PO_4)_2$,[10] $Na_7Cu_4(AsO_4)_5$,[11] and $BaCuAs_2O_7$.[12] Typical magnetic interactions observed have been attributed to the electron coupling through the M−O−M superexchange pathway, instead of through the closed-shell, nonmagnetic oxy anions via the M−O−X−O−M linkages.

A wealth of oxy compounds of the $AMXO_4$ type is known for a number of transition metal (M) cations. A number of phosphates and few arsenates studied adopt the $A^IM^{II}X^VO_4$ form where A^I = alkali metal cation, NH_4^+, Ag^+, Tl^+; M^{II} = Mn, Fe, Ni, Cu, Zn; and X^V = P, As.[5] The title compound $NaCuAsO_4$, **1**, exhibits a new structure type that consists of discrete Cu−O−Cu frameworks. A close comparison with a recently discovered salt-inclusion compound $Na_4ACu_4(AsO_4)_4Cl_2$ (A = Rb, Cs),[13] **2**, shows that both compounds contain tetrameric clusters of four antiferromagnetically coupled Cu^{2+} cations in distinctive shape and geometry, e.g., $[Cu_4O_{16}]^{24-}$ and $[Cu_4O_{12}]$,$^{16-}$ respectively. Hereinafter, we report the synthesis, structure, UV−vis spectroscopy, and magnetic properties of $NaCuAsO_4$. In addition, we will briefly illustrate the correlation in chemistry and structure between **1** and **2**.

Experimental Section

Materials. NaBr (Acros, 99.5%), CsBr (Alfa, 99%), NaCl (EM, GR), RbCl (Strem, 99.8%), As_2O_5 (Aesar, 99.9%), $Cu(OH)_2$ (Alfa, 94%), CuO (Strem, 99.999%), $CuBr_2$ (Strem, 99%), Na_2O_2 (Aldrich, 97%), Cs_2O (Strem, 99%), and Na_2CO_3 (Mallinckrodt, AR) were used.

Single Crystal Growth. Single crystals of $NaCuAsO_4$ were grown from a eutectic flux of 38% NaBr and 62% CsBr, which has a melting point of 460 °C. The data crystal was retrieved originally from the reaction containing the mixture of As_2O_5 (0.4286 mmol), CuO (1 mmol), $CuBr_2$ (0.1429 mmol), Na_2O_2 (0.1429 mmol), and Cs_2O (0.1429 mmol). The reactants were mixed together in a nitrogen-purged drybox and ground in a 1:5 ratio by weight with predried flux. The reaction mixture was placed in a carbon-coated silica ampule, which was then sealed and heated under vacuum. The temperature was raised at a slow rate (20−25 °C) to 300 °C and maintained at a constant for a day, followed by an increase to an isotherm at 650 °C for 4 days. The final reaction step involved slow cooling at 2.5 °C/h to 450 °C followed by cooling at 30 °C/h to room temperature. The products, which contain a 50:50 mixture of dark blue powder, and transparent, pale-green parallelepiped crystals, were retrieved from the flux by washing with deionized water using the suction filtration method. On the basis of the powder X-ray diffraction (PXRD) pattern, the dark blue powder was identified as $NaCu_4(AsO_4)_3$.[6] Both single crystal indexing and PXRD determined that the latter was $NaCuAsO_4$.

It was noticed that the window of reaction temperatures is rather narrow due to the coexistence of $NaCu_4(AsO_4)_3$. Increasing the reaction temperature to 725 and 800 °C might result in larger crystals, but it gives rise to a lower-yield product and poor quality crystals of the title compound.

Stoichimetric Synthesis. The polycrystalline phase can be prepared both in conditions exposed to the air and in sealed quartz ampules. In a typical reaction, a stoichiometric mixture of As_2O_5 (2 mmol), $Cu(OH)_2$ (4 mmol), Na_2CO_3 (2 mmol), NaCl (1 mmol), and RbCl (1 mmol) was heated at 650 °C for 4 days followed by air quenching. On the basis of the PXRD, the final products contained $NaCuAsO_4$ and salt. The pure phase was isolated using washing and the suction filtration method.

Elemental Analysis. Qualitative analysis on the data crystal was carried out by EDAX and showed the presence of the respective elements.

Single Crystal X-ray Structure Determination. Pale-green, parallelepiped crystals were physically examined and selected under an optical microscope equipped with a polarizing light attachment. The data crystal was mounted on glass fiber with epoxy for the X-ray diffraction study. The data were collected at room temperature on a Rigaku AFC-7R four-circle diffractometer (Mo Kα, λ = 0.71073 Å) equipped with a graphite monochromator. Crystallographic data of the title compound are given in Table 1. The final cell parameters were determined by least-squares fit of 25 reflections selected from random search with $53.98° < 2\theta < 54.91°$. Data were collected using an $\omega-2\theta$ scan mode at 16°/min (8 rescans). A total of 1780 reflections ($2\theta_{max} = 55°$) were collected on a primitive cell from two octants ($0 \le h \le 7$, $0 \le k \le 14$, $-13 \le l \le 13$), of which reflections with $F > 2\sigma(F)$ were used for the structural solution. No detectable decay was observed during the data collection, according to the intensities of the three standard reflections (2, −1, 1; 1, −2, −1; 1, −3, 1) measured every 100 reflections. Lorentz-polarization and empirical absorption corrections[14] (ψ scans) were applied to the data. On the basis of Laue class 2/*m* and extinction conditions, the structure was solved in the space group $P2_1/c$ (No. 14). The structure was solved by direct methods with SHELX-95[15] and refined on $|F|^2$ with SHELXTL-Plus.[16] Scattering factors for all atoms were taken from the source

Table 1. Selected Crystal and Refinement Data for $NaCuAsO_4$

empirical formula	$NaCuAsO_4$
fw	225.45
space group, *Z*	$P2_1/c$ (No. 14), 8
T, °C	25
a, Å	6.002(1)
b, Å	10.853(2)
c, Å	10.373(2)
β, deg	91.50(3)
V, Å^3	675.4(2)
μ (Mo Kα), mm^{-1}	16.16
d_{calcd}, g cm^{-3}	4.434
data/restraints/params	1541/0/128
secondary extinction	0.040(1)
final R1/wR2[a] [$I > 2\sigma(I)$]/GOF	0.0275/0.0702/1.18

[a] $R1 = \sum||F_o| - |F_c||/\sum|F_o|$; $wR2 = [\sum w(|F_o| - |F_c|)^2/\sum w|F_o|^2]^{1/2}$; $w = 1/[\sigma^2(F_o^2) + (0.0406P)^2 + 1.1536P]$, where $P = (F_o^2 + 2F_c^2)/3$.

(4) Huang, Q.; Hwu, S.-J. *Inorg. Chem.* **1998**, *37*, 5869−5874.
(5) Ulutagay-Kartin, M.; Etheredge, K. M. S. G.; Schimek, G. L.; Hwu, S.-J. *J. Alloys Compd.* **2002**, *338*, 80−86 and references therein.
(6) Wardojo, T. A.; Mackay, R.; Hwu, S.-J.; Li, S.; O'Connor, C. J.; Pennington, W. T. *Inorg. Chem.*, manuscript in preparation.
(7) Mackay, R.; Wardojo, T. A.; Hwu, S.-J. *J. Solid State Chem.* **1996**, *125*, 255−260.
(8) Etheredge, K. M. S.; Hwu, S.-J. *Inorg. Chem.* **1995**, *34*, 1495−1499.
(9) Etheredge, K. M. S. Ph.D. Dissertation, Rice University, Houston, TX, 1996.
(10) Etheredge, K. M. S.; Hwu, S.-J. *Inorg. Chem.* **1996**, *35*, 1474−1477.
(11) Wardojo, T. A. M.S. Thesis, Rice University, Houston, TX, 1996.
(12) Wardojo, T. A.; Hwu, S.-J. *J. Solid State Chem.* **1995**, *118*, 280−284.
(13) (a) Hwu, S.-J.; Ulutagay-Kartin, M.; Clayhold, J. A.; Mackay, R.; Wardojo, T. A.; O'Connor, C. J.; Krawiec, M. *J. Am. Chem. Soc.* **2002**, *124*, 12404−12405. (b) Clayhold, J. A.; Ulutagay-Kartin, M.; Hwu, S.-J.; Koo, H.-J.; Whangbo, M.-H.; Voigt, A.; Eaiprasertsak, K. *Phys. Rev. B* **2002**, *66*, 052403.
(14) North, A. C.; Phillips, D. C.; Mathews, F. S. *Acta Crystallogr.* **1968**, *A24*, 351−359.

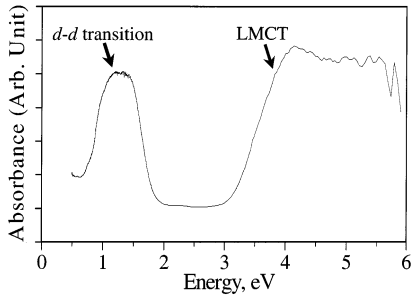

Figure 1. UV−vis spectrum of $NaCuAsO_4$.

Table 2. Atomic Coordinates and Isotropic-Equivalent Displacement Parameters for $NaCuAsO_4$

atom	Wyckoff position	*x*	*y*	*z*	U_{eq} (Å^2)[a]
As(1)	4e	0.12500(5)	0.12101(3)	0.82402(3)	0.0066(1)
As(2)	4e	0.62465(5)	0.36418(3)	0.90753(3)	0.0062(1)
Cu(1)	4e	0.63009(7)	0.39840(4)	0.21983(4)	0.0110(2)
Cu(2)	4e	0.84769(7)	0.61797(4)	0.98949(4)	0.0091(2)
Na(1)	4e	0.8744 (2)	0.1505(2)	0.1182(1)	0.0162(3)
Na(2)	4e	0.3706(2)	0.1290(2)	0.1161(2)	0.0201(4)
O(1)	4e	0.1297(4)	0.1999(2)	0.6838(2)	0.0113(5)
O(2)	4e	0.1175(4)	0.2159(2)	0.9526(2)	0.0118(5)
O(3)	4e	0.5950(4)	0.2971(2)	0.0517(2)	0.0107(5)
O(4)	4e	0.8521(4)	0.4560(2)	0.9125(2)	0.0095(5)
O(5)	4e	0.8943(4)	0.0316(2)	0.8324(2)	0.0105(5)
O(6)	4e	0.6541(4)	0.2664(2)	0.7855(2)	0.0125(5)
O(7)	4e	0.3581(4)	0.0346(2)	0.8438(2)	0.0119(5)
O(8)	4e	0.3849(4)	0.4452(2)	0.8754(2)	0.0097(1)

[a] Equivalent isotropic *U* defined as one-third of the trace of the orthogonalized U_{ij} tensor.

program. The axial photos showed no evidence of superstructure. The positional and thermal parameters for the title compound are listed in Table 2. The selected bond distances and angles are in Table 3.

UV−Vis Diffuse Reflectance Spectroscopy. An optical absorption spectrum of the title compound (Figure 1) was acquired from a PC-controlled SHIMADZU UV-3100 UV−vis−NIR spectrometer equipped with an integrating sphere. $BaSO_4$ was used as a reflectance standard. The UV−vis diffuse reflectance spectrum of the title compound was taken in the range 200 nm (6.2 eV) to 2500 nm (0.5 eV). Data were collected in reflectance (%*R*) mode and manually converted to arbitrary absorption units (α/s) by the relationship $A = \alpha/s$.[17]

Magnetic Susceptibility. Magnetic susceptibility was measured with a Quantum Design SQUID MPMS-5S magnetometer. The measurements were taken from 2 to 300 K in the applied field of H = 1 T. Selected single crystals (6.7 mg) were contained in a gel capsule sample holder. The magnetic susceptibility was corrected for the gel capsule and core diamagnetism with Pascal's constants.[18]

Results and Discussion

Structure Description. The projected view shown in Figure 2 reveals the extended framework of $NaCuAsO_4$ adopting a pseudo-one-dimensional channel structure where the Na^+ cations reside. In the middle of the drawing, it shows a window of oxide anions coordinated to six Cu^{2+} and four As^{5+} cations around the immediate proximity of the sodium cations. The framework consists of the $[Cu_4O_{16}]^{24-}$ tetrameric clusters (see the one in the circled area). Each tetramer is made of four CuO_5 units in a chairlike configuration (Figure 3, right) centered by a center of inversion. The nanostructured

Table 3. Selected Bond Distances (Å) and Angles (deg) for $NaCuAsO_4$

	[CuO_5] Trigonal Bipyramid		
Cu(1)−O(3)	2.068(2)	Cu(2)−O(1)^d	2.013(2)
Cu(1)−O(5)^a	2.088(2)	Cu(2)−O(2)^e	1.910(3)
Cu(1)−O(6)^a	1.918(3)	Cu(2)−O(4)	1.932(3)
Cu(1)−O(7)^b	2.226(2)	Cu(2)−O(4)^e	2.197(2)
Cu(1)−O(8)^c	1.965(2)	Cu(2)−O(8)^c	2.118(2)
O(3)−Cu(1)−O(5)^a	136.43(9)	O(1)^d−Cu(2)−O(2)^e	81.6(1)
O(3)−Cu(1)−O(6)^a	79.0(1)	O(1)^d−Cu(2)−O(4)	91.8(1)
O(3)−Cu(1)−O(7)^b	126.93(9)	O(1)^d−Cu(2)−O(4)	120.1(1)
O(3)−Cu(1)−O(8)^c	91.9(1)	O(1)^d−Cu(2)−O(8)^c	142.7(1)
O(5)^a−Cu(1)−O(6)^a	95.3(1)	O(2)^e−Cu(2)−O(4)^e	170.6(1)
O(5)^a−Cu(1)−O(7)^b	96.64(9)	O(2)^e−Cu(2)−O(4)	96.8(1)
O(5)^a−Cu(1)−O(8)^c	89.5(1)	O(2)^e−Cu(2)−O(8)^c	99.6(1)
O(6)^a−Cu(1)−O(7)^b	98.6(1)	O(4)−Cu(2)−O(4)^e	80.7(1)
O(6)^a−Cu(1)−O(8)^c	170.5(1)	O(4)−Cu(2)−O(8)^c	89.7(1)
O(7)^b−Cu(1)−O(8)^c	89.05(9)	O(4)^e−Cu(2)−O(8)^c	97.02(9)
	[AsO_4] Tetrahedra		
As(1)−O(1)	1.689(2)	As(2)−O(3)	1.676(2)
As(1)−O(2)	1.686(2)	As(2)−O(4)	1.690(2)
As(1)−O(5)	1.695(2)	As(2)−O(6)	1.665(2)
As(1)−O(7)	1.693(2)	As(2)−O(8)	1.712(2)
O(1)−As(1)−O(2)	111.9(1)	O(3)−As(2)−O(4)	109.5(1)
O(1)−As(1)−O(5)	111.5(1)	O(3)−As(2)−O(6)	114.7(1)
O(1)−As(1)−O(7)	110.7(1)	O(3)−As(2)−O(8)	106.8(1)
O(2)−As(1)−O(5)	105.7(1)	O(4)−As(2)−O(6)	107.3(1)
O(2)−As(1)−O(7)	106.4(1)	O(4)−As(2)−O(8)	112.2(1)
O(5)−As(1)−O(7)	110.5(1)	O(6)−As(2)−O(8)	106.6(1)
	[Na(1)O_6] Polyhedra		
Na(1)−O(1)^a	2.322(3)	Na(1)−O(5)^f	2.461(3)
Na(1)−O(2)	2.390(3)	Na(1)−O(6)^a	2.386(3)
Na(1)−O(3)	2.400(3)	Na(1)−O(7)^f	2.483(3)
O(1)^a−Na(1)−O(2)	65.96(9)	O(2)−Na(1)−O(7)^f	135.3(1)
O(1)^a−Na(1)−O(3)	94.1(1)	O(3)−Na(1)−O(5)^f	168.0(1)
O(1)^a−Na(1)−O(5)^f	97.9(1)	O(3)−Na(1)−O(6)^a	64.04(9)
O(1)^a−Na(1)−O(6)^a	84.1(1)	O(3)−Na(1)−O(7)^f	100.99(9)
O(1)^a−Na(1)−O(7)^f	152.7(1)	O(5)^f−Na(1)−O(6)	118.2(1)
O(2)−Na(1)−O(3)	91.8(1)	O(5)^f−Na(1)−O(7)^f	68.51(9)
O(2)−Na(1)−O(5)^f	92.08(9)	O(6)^a−Na(1)−O(7)^f	82.29(9)
O(2)−Na(1)−O(6)^a	140.4(1)		
	[Na(2)O_8] Polyhedra		
Na(2)−O(1)^b	2.468(3)	Na(2)−O(6)^a	2.668(3)
Na(2)−O(2)^g	2.437(3)	Na(2)−O(7)^f	3.004(3)
Na(2)−O(3)	2.375(3)	Na(2)−O(7)^g	2.437(3)
Na(2)−O(5)^h	2.427(3)	Na(2)−O(8)^a	2.807(3)
O(1)^b−Na(2)−O(2)^g	63.07(9)	O(3)−Na(2)−O(6)^a	60.09(8)
O(1)^b−Na(2)−O(3)	80.9(1)	O(3)−Na(2)−O(7)^g	89.88(9)
O(1)^b−Na(2)−O(5)^h	94.9(1)	O(3)−Na(2)−O(7)^f	103.1(1)
O(1)^b−Na(2)−O(6)^a	81.98(9)	O(3)−Na(2)−O(8)^a	119.14(9)
O(1)^b−Na(2)−O(7)	153.3(1)	O(5)^h−Na(2)−O(6)^a	124.8(1)
O(1)^b−Na(2)−O(7)	121.58(9)	O(5)^h−Na(2)−O(7)^f	83.0(1)
O(1)^b−Na(2)−O(8)^a	86.95(9	O(5)^h−Na(2)−O(7)^g	87.80(9)
O(2)^g−Na(2)−O(3)	81.62(9)	O(5)^h−Na(2)−O(8)^a	65.63(8)
O(2)^g−Na(2)−O(5)^h	91.76(9)	O(6)^a−Na(2)−O(7)^f	77.63(9)
O(2)^g−Na(2)−O(6)^a	132.0(1)	O(6)^a−Na(2)−O(7)^g	139.86(9)
O(2)^g−Na(2)−O(7)^f	143.4(1)	O(6)^a−Na(2)−O(8)^a	59.21(8)
O(2)^g−Na(2)−O(7)^g	58.51(8)	O(7)^f−Na(2)−O(7)^g	84.98(9)
O(2)^g−Na(2)−O(8)^a	141.3(1)	O(7)^f−Na(2)−O(8)^a	67.91(8)
O(3)−Na(2)−O(5)^h	173.3(1)	O(7)^g−Na(2)−O(8)^a	143.40(9)

[a] $x, -y + 1/2, z + 1/2$. [b] $x - 1, -y + 1/2, z + 1/2$. [c] $-x + 1, -y + 1, -z + 2$. [d] $-x + 2, y + 1/2, -z + 3/2$. [e] $-x + 2, -y + 1, -z + 2$. [f] $-x + 2, -y, -z + 2$. [g] $x - 1, y, z$. [h] $-x + 1, -y, -z + 2$.

(15) Sheldrick, G. M. In *Crystallographic Computing 3*; Sheldrick, G. M., Kruger, C., Goddard, R., Eds.; Oxford University Press: London, 1985; pp 175−189.
(16) Sheldrick, G. M. In *SHELXTL, Version 6.1 Structure Determination Software Programs*; Bruker Analytical X-ray Systems Inc.: Madison, WI, 1997−2001.
(17) (a) Kubelka, P.; Munk, F. Z. *Tech. Phys.* **1931**, *12*, 593. (b) Kubelka, P. *J. Opt. Soc. Am.* **1948**, *38*, 448−457.
(18) O'Connor, C. J. *J. Prog. Inorg. Chem.* **1982**, *29*, 203−276.

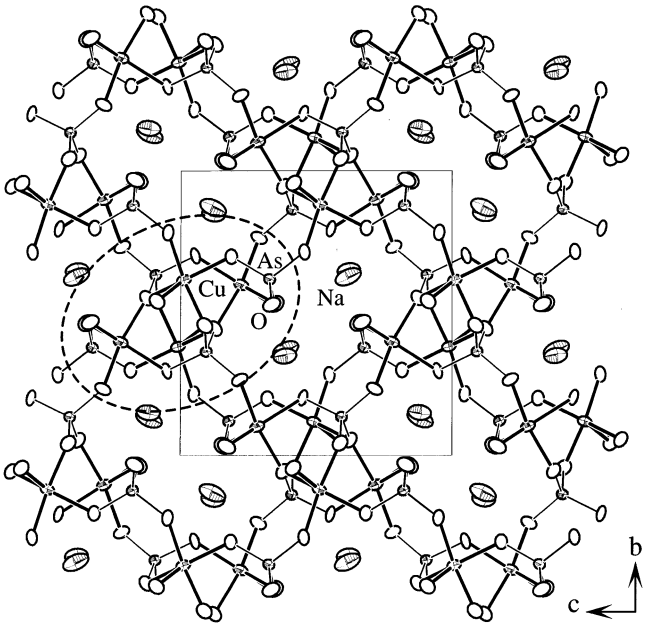

Figure 2. Projected view showing the structure of $NaCuAsO_4$ along *a*-axis. One of the $[Cu_4O_{16}]^{24-}$ clusters is located in the area outlined by a dotted circle. The clusters center around the edge-center of the unit cell. The Cu−O bonds are drawn in thick lines, and As−O in thin lines. No Na−O bonds were shown for clarity. The atoms were drawn at 95% probability.

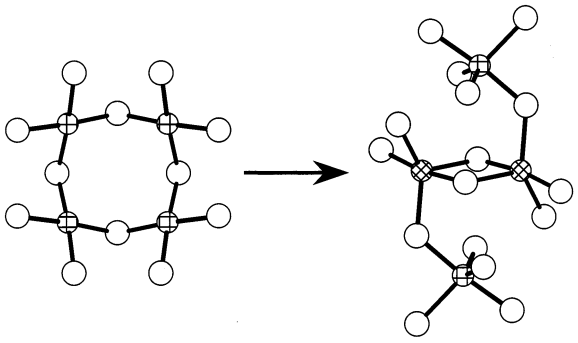

Figure 3. Tetrameric clusters found in the structures of $Na_4ACu_4(AsO_4)_4Cl_2$ (left, ref 13a) and $NaCuAsO_4$ (right). Throughout the article, the crosshatched circles represent copper. For the latter, Cu(1) is drawn in vertical/horizontal crosses and Cu(2) in slanted lines. The arrow represents the conversion via thermal decomposition at 900 °C (see text).

tetramer-containing compound can be isolated via the thermal decomposition of previously reported $Na_4ACu_4(AsO_4)_4Cl_2$ (A = Rb, Cs).[13a] The latter also contains a tetrameric cluster of four antiferromagnetically coupled Cu^{2+} ions in different geometry, $[Cu_4O_{12}]^{16-}$ (Figure 3, left). Both compounds are currently under investigation by neutron inelastic scattering methods and band-structure calculations for their unusual magnetic properties, including spin gap formation.[19] In the following sections, therefore, we will continue our discussions on the title compound with respect to its structure connectivity, local geometry, and oxidation states of ions concerning the phenomena associated with the observed electronic and magnetic properties.

The $[Cu_4O_{16}]^{24-}$ magnetic clusters interlink through closed-shell, nonmagnetic AsO_4^{3-} oxy anions to form the three-dimensional network. Figure 4 shows that the $[Cu_4O_{16}]^{24-}$ clusters are well spaced by the AsO_4^{3-} tetrahedral units. All the unshared oxygen atoms in this drawing partake the formation of the Cu−O−As linkages.

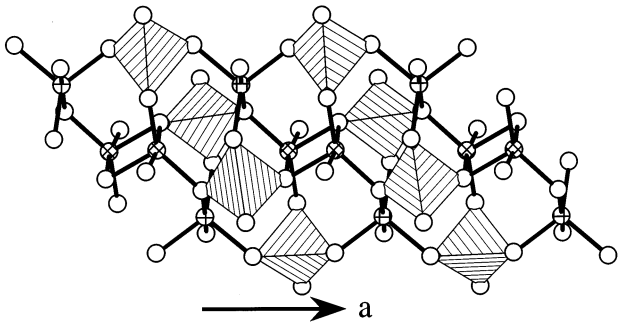

Figure 4. Ball-and-stick and polyhedral composite representation showing partial structure of the Cu−As−O framework. The polyhedral units represent As-centered oxygen tetrahedra.

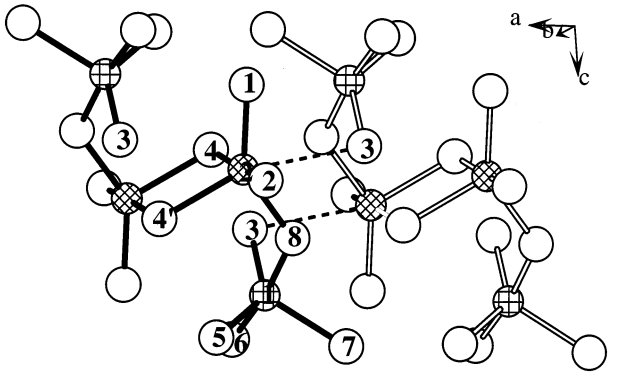

Figure 5. Two $[Cu_4O_{16}]^{24-}$ clusters showing the intercluster interaction through the long Cu(2)−O(3) bonds (dotted lines). To distinguish the two tetramers, one is highlighted with solid Cu−O bonds and the other in hollow bonds.

All the Cu−O bond distances indicate much stronger intracluster than intercluster interactions. As shown in Figure 5, each cluster consists of a pair of edge-shared $Cu(2)O_5$ with two $Cu(1)O_5$ units sharing vertex oxygen atoms at opposite ends. The Cu−O bonds for the distorted square-pyramidal CuO_5 units range from 1.91 to 2.23 Å, see Table 3. The Cu−O distances for the basal-plane oxygen atoms are quite uniform, e.g., 1.92−2.09 Å for $Cu(1)O_5$ and 1.91−2.12 Å for $Cu(2)O_5$. Those of the apical Cu(1)−O(7) and Cu(2)−O(4′) bonds, however, are on the long side, e.g., 2.23 and 2.20 Å, respectively. The basal distances are consistent with the sum of Shannon crystal radii, 2.01 Å, of five-coordinated Cu^{2+} (0.79 Å) and O^{2-} (1.22 Å),[20] as well as those in the reported copper(II) phosphates and arsenates.[5] In any event, the shortest intracluster Cu(2)−O(3) distance facing the distorted O(1,2,4′,4) plane is much too long, e.g., 3.51 Å, to be considered a bond (Figure 5). However, the intercluster Cu(2)−O(3) bonds (dotted lines) adopt a relatively shorter distance of 2.83 Å and a much distorted apical angle ∠O(4′)−Cu(2)−O(3) of 160.5°. While both Cu^{2+} cations adopts the [4 + 1] Jahn−Teller distortion, the coordination of Cu(2) could be considered the [4 + 2] type taking into account the extra Cu−O intercluster interaction.

(19) Nagler, S. E.; Whangbo, M.-H.; Clayhold, J. A.; Ulutagay-Kartin, M.; Hwu, S.-J. Unpublished results, 2002.

(20) Shannon, R. D. *Acta Crystallogr.* **1976**, *A32*, 751−767.

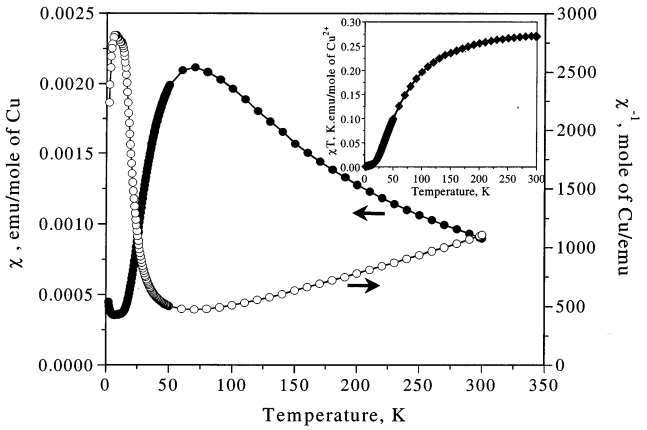

Figure 6. Temperature-dependent magnetic susceptibility of $NaCuAsO_4$.

For the spin coupling between the Cu^{2+} d^9 cations, there are potentially four superexchange pathways within each cluster, i.e., 2×Cu(1)−O(8)−Cu(2) and 2×Cu(2)−O(4)−Cu(2). The latter corresponds to the edge-shared $Cu(2)O_5$ units, with the bond angle of 99.34°. The angle for corner-shared $Cu(1,2)O_5$ is 126.2°. Both bond angles are well within the range for the antiferromagnetic spin couplings.[21]

The bond valence sum (BVS) analysis confirms the oxidation states of the Na^+, Cu^{2+}, and As^{5+} cations.[22] The Na−O bond distances (Table 3) used for the calculations are 2.32−2.48 Å for the six-coordinated $Na(1)O_6$ and 2.38−3.00 Å for the eight-coordinated $Na(2)O_8$ polyhedra resulting in the values of +1.19 and +1.13, respectively. Also, two independent AsO_4 tetrahedra adopt rather uniform bond distances, 1.67−1.71 Å, which result in the BVS values of +4.92 for As(1) and +4.99 for As(2). The corresponding values for the two independent coppers are +1.90 for Cu(1) and +2.00 for Cu(2) as expected, on the basis of the CuO_5 coordination.

UV−Vis Diffuse Reflectance. The electronic absorption spectrum of the title compound exhibits two bands almost in equal intensity (Figure 1). The absorption above 3.2 eV can be assigned to the LMCT (ligand-to-metal charge transfer) bands originated from the AsO_4 oxy anion. These bands are comparable with the values acquired in earlier studies.[13,23] The ligand-field spectra show a rather intense absorption band centered around 1.3 eV corresponding to the otherwise Laporte-forbidden, d−d transition. The intense absorption is consistent with the much-distorted [4 + 1] and [4 + 2] coordination around the Cu^{2+} cations.

Magnetic Susceptibility. The temperature dependence of the magnetic susceptibility, χ, of the title compound, along with its inverse susceptibility, χ^{-1}, is shown in Figure 6. The inset shows a graph of χT. The susceptibility data appear to be consistent with local-cluster antiferromagnetism. At high temperatures, the χT data indicate that the susceptibility approaches a pure Curie law, suggesting weakly interacting spins, but with a rapid suppression of the effective spin below $T = 70$ K. At low temperature, the susceptibility collapses as the local magnetic clusters settle into the lowest energy magnetic singlet state. Attempts to fit the data to models of extended, noncluster magnetism were inconclusive because there was significant curvature in χ^{-1} at all temperatures and the Curie−Weiss fits to the inverse susceptibility failed to yield a unique value for the Weiss constant, θ. From the asymptotic, high-temperature value of χT, we can extract an effective value for the magnetic moment, $\mu_{eff} = 1.98\ \mu_B$, consistent with crystal-field quenching of orbital magnetism. The superexchange interactions between distinct $[Cu_4O_{16}]^{24-}$ units appear to be much weaker than the interactions within the same unit. The magnetic behavior of $NaCuAsO_4$ appears to essentially be that of discrete clusters of four antiferromagnetically coupled Cu^{2+} ions. Detailed results of theoretical band-structure calculations and neutron studies showing the origin of magnetic behaviors will be published elsewhere.[19]

In a final remark, the present studies in the exploratory synthesis of quasi-low-dimensional transition-metal-based oxy compounds give a new perspective to the continued investigation of new materials for experimental and theoretical developments of magnetic models. The resulting nanostructured tetramers can be considered discrete magnetic clusters for they are confined in an oxide matrix made of closed-shell, nonmagnetic oxy anions, AsO_4^{3-} in this case. The tetrameric unit shown in this report draws a close comparison with that of a recently discovered salt-inclusion compound $Na_4ACu_4(AsO_4)_4Cl_2$ (A = Rb, Cs), in that both magnetic clusters contain four antiferromagnetically coupled Cu^{2+} cations, namely $[Cu_4O_{16}]^{24-}$ and $[Cu_4O_{12}]^{16-}$, respectively. We anticipate that the ongoing investigation of structure and property correlation via neutron scattering and band-structure calculations would help us reveal the spin interactions in clusters of different geometry. The title compound represents a new structure type that consists of discrete Cu−O−Cu frameworks, and we anticipate more compounds containing nanostructured magnetic clusters of different size, shape, and symmetry are yet to come.

Acknowledgment. We gratefully acknowledge continued financial support from the National Science Foundation (Grants DMR-0077321 and EPS-9977797 for the research, CHE-9808044 for the purchase of SQUID magnetometer, and ESR-9108772, CHE-9207230, and CHE-9808165 for the purchase of X-ray instrumentation). The authors are also in debt to Dr. M. Krawiec for his assistance on X-ray structure analysis. M.U.-K. thanks the Turkish Government and Balikesir University for partial financial support.

Supporting Information Available: X-ray crystallographic file, in CIF format, including tables of crystallographic details, atomic coordinates, anisotropic thermal parameters, and interatomic distances and angles. This material is available free of charge via the Internet at http://pubs.acs.org.

IC026169Q

(21) Hay, P. J.; Thibeault, J. C.; Hoffmann, R. *J. Am. Chem. Soc.* **1975**, *97* (17), 4884−4899.
(22) Brown, I. D.; Altermatt, D. *Acta Crystallogr.* **1985**, *B41*, 244−247.
(23) (a) Ulutagay, M.; Schimek, G. L.; Hwu, S.-J.; Taye, H. *Inorg. Chem.* **1998**, *37*, 1507−1512. (b) Ulutagay, M.; Schimek, G. L.; Hwu, S.-J. *Acta Crystallogr.* **1998**, *C54*, 898−900. (c) Ulutagay, M. M.S. Thesis, Clemson University, Clemson, SC, 1997.